

2007

Impact of sintering temperature on the physical properties of the superconducting ferromagnet: RuSr₂Eu_{1.5}Ce_{0.5}Cu₂O₁₀

Rashmi Nigam

University of Wollongong, rnigam@uow.edu.au

Alexey V. Pan

University of Wollongong, pan@uow.edu.au

S X. Dou

University of Wollongong, shi@uow.edu.au

Follow this and additional works at: <https://ro.uow.edu.au/engpapers>



Part of the [Engineering Commons](#)

<https://ro.uow.edu.au/engpapers/4024>

Recommended Citation

Nigam, Rashmi; Pan, Alexey V.; and Dou, S X.: Impact of sintering temperature on the physical properties of the superconducting ferromagnet: RuSr₂Eu_{1.5}Ce_{0.5}Cu₂O₁₀ 2007, 09G109-1-09G109-3.
<https://ro.uow.edu.au/engpapers/4024>

Research Online is the open access institutional repository for the University of Wollongong. For further information contact the UOW Library: research-pubs@uow.edu.au

Impact of sintering temperature on the physical properties of the superconducting ferromagnet: $\text{RuSr}_2\text{Eu}_{1.5}\text{Ce}_{0.5}\text{Cu}_2\text{O}_{10}$

R. Nigam,^{a)} A. V. Pan, and S. X. Dou

Institute for Superconducting and Electronic Materials, University of Wollongong, NSW 2522, Australia

(Presented on 10 January 2007; received 27 October 2006; accepted 4 December 2006; published online 25 April 2007)

We report the influence of the sintering temperature on the electromagnetic behavior for the $\text{RuSr}_2\text{Eu}_{1.5}\text{Ce}_{0.5}\text{Cu}_2\text{O}_{10}$ material, in which superconductivity and ferromagnetism coexist. The inadequate heat treatment results in the coexistence of the secondary Ru-1212 phase along with the dominant Ru-1222 phase. The presence of two phases leads to the magnetic superposition of the signals from both phases, which results in the observation of a small peak around 120–130 K. In the pure Ru-1222 no such magnetic anomaly is observed. In addition, the impure samples exhibit a double step superconductivity transition. In the normal state, these impure samples exhibit a semiconductinglike behavior of the resistivity. In contrast, the pure Ru-1222 sample with much larger, well connected grains has a single step resistivity transition, as well as a metalliclike behavior in the normal state. Our work sends a strong message that only high quality, phase pure samples can be chosen for the investigation of the complex behavior in the Ru system. © 2007 American Institute of Physics. [DOI: 10.1063/1.2710451]

The recent discovery of the coexistence of superconductivity and ferromagnetism in ruthenocuprates, such as $\text{RuSr}_2\text{R}_{2-x}\text{Ce}_x\text{Cu}_2\text{O}_{10}$ (Ru-1222) (Refs. 1 and 2) and $\text{RuSr}_2\text{RCu}_2\text{O}_8$ (Ru-1212) (Refs. 3 and 4) (where $R=\text{Eu}$, Gd, and Sm), has generated a lot of interest. In these compounds superconductivity appears when the system is in ferromagnetic state, hence they are called superconducting ferromagnets (SCFM). In Ru-1212, magnetic transition is observed at $T_M=133$ K and superconductivity sets in at 35 K.^{3,4} Ru-1222 display magnetic transition at 125–180 K and the superconductivity below 32–50 K.^{1,2,5,9}

The present work focuses on the Ru-1222 system. The Ru-1222 compound has a complicated magnetic behavior. The material has been found to be paramagnetic at room temperature but as it is cooled down, it undergoes antiferromagnetic transition,^{1,2,5} followed by spin glass behavior⁶ and ferromagnetic transition.^{1,2,5} Below the ferromagnetic transition, the superconductivity sets in and coexists with the ferromagnetism. Despite numerous studies, the exact nature of magnetic ordering is still unknown for the Ru-1222 system.⁵

The phase purity of Ru-1222 system is a critical aspect in understanding the true superconducting, magnetic and transport properties of this material. In this work, the influence of sintering temperature on the phase purity of Ru-1222 samples is elucidated. It has been observed that the Ru-1212 phase exists as an impurity in bulk Ru-1222 material at relatively low sintering temperatures. Elevating the sintering temperature leads to decomposition of the Ru-1212 phase. The corresponding variation in structural, superconducting, magnetic, and transport properties has been observed and discussed in detail.

The samples of $\text{RuSr}_2\text{Eu}_{1.5}\text{Ce}_{0.5}\text{Cu}_2\text{O}_{10}$ (Ru-1222) were synthesized through a solid state reaction route from the sto-

ichiometric amounts of 99.99% pure RuO_2 , SrCO_3 , Eu_2O_3 , CeO_2 , and CuO . Three different samples with the same stoichiometry were prepared with the same intermediate heat treatment of 1000, 1020, and 1040 °C for 12 h, but different final sintering temperatures of 1060, 1080, and 1090 °C. The samples were pressed into circular pellets. The pellet of 1060 °C-sintered powder was sintered again at 1060 °C, whereas those of 1080 °C- and 1090 °C-sintered powders were sintered at the common temperature of 1070 °C. The $\text{RuSr}_2\text{EuCu}_2\text{O}_8$ (Ru-1212) sample was also prepared using the same procedure mentioned above but with the final sintering temperature of 1080 °C. All the pellets were then annealed in flowing oxygen at 600 °C for 48 h and subsequently cooled over a span of another 24 h down to room temperature. $\text{RuSr}_2\text{Eu}_{1.5}\text{Ce}_{0.5}\text{Cu}_2\text{O}_{10}$ samples thus obtained are named 1060 °C-, 1080 °C-, and 1090 °C-sintered samples.

The XRD pattern of the Ru-1222 sample (Fig. 1), which was sintered at 1060 °C, shows a large number of impurity phases. These unidentified impurity phases have also been found in Ref. 7 and the sample has been claimed as nearly single phase (~97%). However, our work shows that these impurity phases have pronounced effect on properties of the Ru-1222 system. Thus, this kind of sample cannot be claimed as nearly single phase if this is used for the elucidation of physical properties. The XRD pattern of 1060 °C-sintered sample was compared with that of Ru-1212. It was clearly observed that (101), (102), (104), (113), and (213) reflections respectively at $2\theta=24.5^\circ$, 39° , 40.7° , 58.8° , and 63° for 1060 °C-sintered sample correspond to the Ru-1212 phase (Fig. 1). This indicates the presence of the considerable amount of Ru-1212 phase along with the desired Ru-1222 phase in the 1060 °C-sintered sample. As can be seen in Fig. 1, increasing the sintering temperature by 20 °C, the impurity peaks disappear. Only a small (213) reflection at $2\theta=16^\circ$ corresponding to Ru-1212 phase is ob-

^{a)}Author to whom correspondence should be addressed; electronic mail: rn393@uow.edu.au

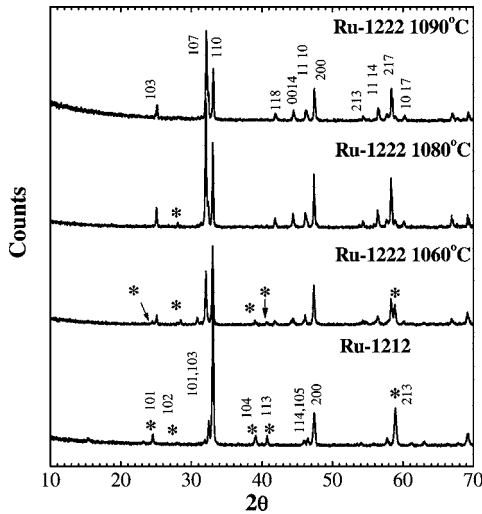


FIG. 1. XRD patterns of Ru-1212 and 1060 °C-, 1080 °C-, and 1090 °C-sintered samples of Ru-1222.

served. The further 10 °C increase in sintering temperature shows no sign of the Ru-1212 phase in the XRD pattern within XRD sensitivity. Ru-1222 belongs to the space group $I4/mmm$ with the lattice parameters $a=b=3.93033$ Å and $c=29.3111$ Å for the 1060 °C sample; $a=b=3.84398$ Å and $c=28.5957$ Å for the 1080 °C sample; and $a=b=3.8458$ Å and $c=28.5919$ Å for the 1090 °C sample. Ru-1212 belongs to the space group $P4/mmm$ with the lattice parameters $a=b=3.84601$ Å and $c=11.5486$ Å.

The zero-field cooled (ZFC) and field cooled (FC) dc magnetization measurements for 1060 °C-sintered (phase impure) and 1090 °C-sintered (phase pure) Ru-1222 samples show a change in slope (a small kink) at about 37 K [Fig. 2(a)] and 25 K [Fig. 2(b)], respectively. This kink corresponds to the superconducting onset temperature, T_c^{onset} . In addition, a clear diamagnetic signal is respectively observed below 10 and 15 K for the impure and pure samples, which indicates the superconducting property of the material. Similar hysteresis loops were obtained for both samples over a

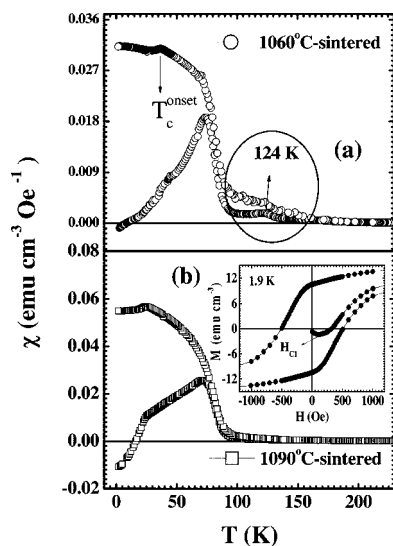


FIG. 2. ZFC-FC susceptibility ($\chi=M/H$) curve obtained at $H=10$ Oe for 1060 and 1090 °C samples. The inset shows magnetization (M) vs applied magnetic field (H) curve at $T=1.9$ K for the 1090 °C-sintered sample.

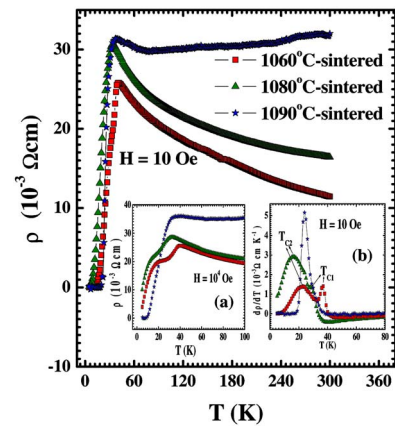


FIG. 3. Resistivity vs temperature curves at $H=10$ Oe. Inset (a) resistivity curves at $H=10^4$ Oe and inset (b) first derivative of resistivity at $H=10$ Oe for the Ru-1222 samples.

wide temperature range. Below 60 K (but above T_c^{onset}), the hysteresis loops start opening up and exhibiting increasing irreversibility with decreasing temperature. This appearance of the irreversibility indicates the transition from soft to hard ferromagnetic behavior at 60 K. Apparently, the ferromagnetic signal also dominates below T_c^{onset} , since the superconducting contribution to the loop irreversibility below T_c^{onset} is hardly noticeable, as can be in the case of a superposition of very strong superconducting and ferromagnetic signals.⁸ However, the coexistence of superconductivity and ferromagnetism can also be evident from the M - H curve at 1.9 K. The ZFC part of the ferromagneticlike hysteresis loop exhibits a Meissner-like linear increase in diamagnetic signal up to 127 Oe, typical for a superconducting state below the first critical field H_{c1} [inset in Fig. 2(b)].

There is one obvious qualitative difference between the $\chi(T)$ behavior of the pure and impure samples, which sheds doubts on the existing explanations on magnetic ordering above approximately 90 K: for the impure sample [Fig. 2(a)], the peak is observed at about 124 K, whereas no such peak is present for the pure sample [Fig. 2(b)]. Additionally, the pronounced irreversibility has been measured within 90–200 K for the impure sample, which is highly suppressed for the pure sample. A similar behavior to that of the impure sample has been reported in Refs. 5, 7, and 11. On the other hand, “no peak” behavior similar to that of the pure sample has been reported in Refs. 1 and 10. However, no explanation on this inconsistency in the Ru-1222 system has been provided. Taking into account the XRD results (Fig. 1), we propose that this peak is merely the result of the existence of the two Ru phases in this system. In the light of this explanation, the understanding of the magnetic behavior in this complex system may need to be revised and will be published elsewhere.¹² In this work, we would like to further emphasize a possible influence of the second phase existing in the Ru-1222 system on transport properties measured.

Figure 3 shows resistivity curve at 10 Oe for the Ru-1222 samples. The 1060 and 1080 °C samples undergo a double superconducting transition, as can be better seen in the first derivative ($d\rho(T)/dT$) of the resistivity shown in inset (b). The first transition (T_{c1}) at a higher temperature and the second transition (T_{c2}) at a lower temperature were de-

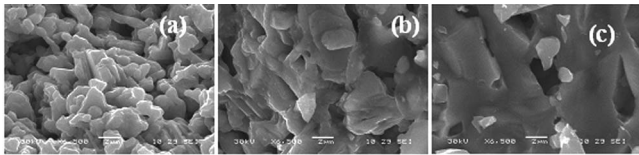


FIG. 4. SEM images of Ru-1222 samples prepared at (a) 1060 °C, (b) 1080 °C, and (c) 1090 °C.

fined at the corresponding peaks in the first derivative [arrows in inset (b) of Fig. 3]. It should be noted that the value of T_c^{onset} obtained from the magnetization experiments (Fig. 2) coincides with T_{c1} measured at the same field. This allows us to attribute T_{c1} to the bulk superconductivity of the dominant Ru-1222 phase and the second transition at T_{c2} , existing in the impure samples only, to the secondary Ru-1212 phase. As can be seen in inset (a) of Fig. 3, the double transition behavior becomes more pronounced at higher fields. A similar double transition behavior has been observed for Bi-2223 polycrystalline superconductors, which contain different fractions of the Bi-2212 superconducting phase.¹⁶ On the other hand, a *single* step superconducting transition could be seen for the 1090 °C sample over the wide field range (Fig. 3). The first derivative shows only one well-pronounced peak for this pure sample. Furthermore, the normal state resistivity is also different for the impure samples, which show a semiconductorlike behavior (exponentially decreasing with temperature), and the pure (1090 °C) sample, exhibiting a metallic behavior, which linearly increases starting from about 75 K. Similar differences in the resistivity have also been found in the literature^{13–15} and have been attributed to the difference in synthesis conditions of the samples.

Another possible explanation to the double step superconducting transition is the granularity of the prepared samples. In this case, the transition to superconducting state takes place via two intermediate stages:¹⁷ (i) the intragranular sharp drop of resistivity at T_{c1} occurs when the grains become superconducting, whereas weak links between the grains contribute nonzero resistance across the entire sample; (ii) at T_{c2} the weak links become superconducting with the Josephson currents forming a three-dimensional (3D) intergranular superconducting network, which leads to the second transition at T_{c2} . In our samples, the SEM observations (Fig. 4) exhibit a well-pronounced granularity for the sample prepared at 1060 °C with relatively small grains (typically 2 μm) and pronounced grain boundaries. This microstructure with small grains and weak intercoupling between grains can also explain the semiconductorlike behavior above T_{c1} . For 1080 °C sample, the grains become larger up to about 5 μm . A further 10 °C enhancement in the sintering temperature for the 1090 °C sample results in almost no isolated grains and in small intergranular regions with hardly distinguishable grain boundaries. This microstructure could lead to strong intergranular coupling and hence a single superconducting transition, as well as to metallic behavior in the normal state.

As the phase formation progresses during the solid state reaction, the secondary phase is known to reside in between the grains of the dominating phase. The most related example can be the Bi-based superconducting system which

possesses at least two main well-studied superconducting phases, so that the formation of the higher- T_c phase (Bi-2223) is always accompanied by the lower- T_c phase (Bi-2212), which can “wrap” around the Bi-2223 grains, creating weak-link boundaries.¹⁷ Our investigations indicates that the double superconducting transition in the impure samples and the normal state resistivity behavior are most likely governed by the combined effect of the granularity revealed in the polycrystalline Ru system and the presence of the secondary Ru-1212 phase reducing the intergranular coupling. In other words, the Ru-1222 grains become superconducting at T_{c1} and the grain boundary region consisting of minority fraction of the Ru-1212 phase becomes superconducting at T_{c2} . In the pure samples, no second phase is present, and the granularity is to a large extent overcome, leading to the single phase transition and metalliclike behavior of the resistivity.

In conclusion, the influence of phase purity and microstructure as a result of the sintering temperature adjustment for $\text{RuSr}_2\text{Eu}_{1.5}\text{Ce}_{0.5}\text{Cu}_2\text{O}_{10}$ is clearly evident in the present study. The sintering temperatures below 1090 °C produce impure Ru-1222 material with a considerable amount of the Ru-1212 phase. An increase in the sintering temperature up to 1090 °C results in decomposition of the Ru-1212 phase, so that nearly single Ru-1222 phase is obtained leading to significantly modified superconducting transition, normal state resistivity, and magnetic behavior of the Ru system. The pronounced irreversibility in ZFC and FC curves and the small peak at 124 K in the impure Ru-1222 are likely to appear due to magnetic interference of the Ru-1212 impurity phase and the bulk Ru-1222 phase. A more detailed study is required to understand the possible influence of these findings on the existing explanation of the magnetic ordering, transitions, and properties in the Ru-1222 system.

The authors are grateful to J. Horvat and V. P. S. Awana for fruitful discussions and interest to the work. This work has been supported by the Australian Research Council.

- ¹I. Felner, U. Asaf, Y. Levi, and O. Millo, *Phys. Rev. B* **55**, R3374 (1997).
- ²E. B. Sonin and I. Felner, *Phys. Rev. B* **57**, 14000 (1998).
- ³C. Bernhard *et al.*, *Phys. Rev. B* **59**, 14099 (1999).
- ⁴A. C. MacLaughlin, W. Zhao, J. P. Attfield, A. N. Fitch, and J. L. Tallon, *Phys. Rev. B* **60**, 7512 (1999).
- ⁵I. Felner, E. Galstyan, and I. Nowik, *Phys. Rev. B* **71**, 064510 (2005).
- ⁶C. A. Cardoso, F. M. Araujo-Moreira, V. P. S. Awana, E. Takayama-Muromachi, O. F. de Lima, H. Yamauchi, and M. Karppinen, *Phys. Rev. B* **67**, 020407 (2003).
- ⁷N. Baclchev, B. Kunev, J. Pirov, G. Mihova, and K. Nenkov, *Mater. Lett.* **59**, 2357 (2005).
- ⁸A. V. Pan, S. Zhou, H. Liu, and S. Dou, *Supercond. Sci. Technol.* **16**, L33 (2003).
- ⁹I. Felner, E. Galstyan, R. H. Herber, and I. Nowik, *Phys. Rev. B* **70**, 094504 (2004).
- ¹⁰I. Felner, E. B. Sonin, T. Machi, and N. Koshizuka, *Physica C* **341–348**, 715 (2000).
- ¹¹A. Shengelaya, R. Khasanov, D. G. Eshchenko, I. Felner, U. Asaf, I. M. Savić, H. Keller, and K. A. Müller, *Phys. Rev. B* **69**, 024517 (2004).
- ¹²R. Nigam, A. V. Pan, and S. X. Dou (unpublished).
- ¹³I. Felner, E. Galstyan, B. Lorenz, D. Cao, Y. S. Wang, Y. Y. Xue, and C. W. Chu, *Phys. Rev. B* **67**, 134506 (2003).
- ¹⁴X. H. Chen, Z. Sun, K. Q. Wang, S. Y. Li, Y. M. Xiong, M. Yu, and L. Z. Cao, *Phys. Rev. B* **63**, 064506 (2001).
- ¹⁵V. P. S. Awana *et al.*, *Physica C* **445–448**, 97 (2006).
- ¹⁶H. Salamati and P. Kameli, *Physica C* **403**, 60 (2004).
- ¹⁷E. A. Early *et al.*, *Phys. Rev. B* **47**, 433 (1993).